Mon. Not. R. astr. Soc. (1972) **159**, 129–153.

OBSERVATIONS OF RECOMBINATION LINES AT DECIMETRE WAVELENGTHS

A. Pedlar and R. D. Davies

(Received 1972 April 24)

SUMMARY

Recombination lines from a total of 15 H II regions have been measured in the 166α (1424·734 MHz), 192α (921·897 MHz) and 220α (613·405 MHz) transitions. A description is given of the observational and reduction techniques; the spectra of all the observed lines are given.

The data from these observations taken with published results of other transitions have been used to derive some of the physical parameters of the H II regions studied. The following deductions have been made from the observations.

(1) Electron temperatures in the range 4000–7000 °K have been derived for the low emission measure H II regions, values significantly less than those of the higher brightness objects.

(2) The non-LTE analysis of Hjellming and Davies has been found to fit the present high quantum number data with only minor modifications.

(3) An apparently lower He/H line ratio for some 220α observations compared with lower n observations is discussed in terms of possible ionization zoning in H II regions.

(4) The observed line broadening suggests that supersonic velocities occur in most of the H II regions studied.

(5) Finally, the line attributed to carbon increases monotonically relative to the hydrogen line as the quantum number increases to 220.

1. INTRODUCTION

Most radio recombination line studies have been made at centimetre wavelengths which correspond to α-transitions ($\Delta n = 1$) at $n \lesssim 150$. This paper reports observations of recombination lines at decimetre wavelengths and therefore at appropriately higher values of n.

For higher n transitions the transition probability decreases, the lines become weaker and are hence more difficult to observe. Dieter (1967) detected the 158α transition in 40 galactic H II regions using an observing beamwidth of 34′ arc. McGee *et al.* (1969) observed the same transition in nine southern sources (12·3′ arc beamwidth) and de Boer *et al.* (1968) observed the 166α transition in six sources (35′ arc beamwidth). Most of the other published observations of these transitions have referred to only a few of the stronger sources, mainly M17 and Orion A. Apart from a single observation of the 253α transition in W80 by Penfield, Palmer & Zuckerman (1967), no α-transitions with $n > 180$ have been reported.

We have extended the range of observed α-transitions by observing the 220α (613·405 MHz), the 192α (921·897 MHz) and the 166α (1424·734 MHz) transitions in a selection of galactic H II regions.

One aim of the observations was to investigate the Stark broadening of the line profiles, which increases as n^7. This has been discussed fully in an earlier paper

(Pedlar & Davies 1971). A second aim was to detect the predicted deviations from local thermodynamic equilibrium (LTE) line intensity and, if possible, to obtain estimates of electron temperatures in the H II regions studied. A third aim was to investigate anomalous recombination lines which appear to be emitted from atoms with a mass $\approx 12M_H$ and which have been detected in several sources at centimetre wavelengths. The present observations contribute to our knowledge of the strength of these lines at higher values of n.

2. THE OBSERVATIONAL AND REDUCTION TECHNIQUES

All observations were carried out using the Mark I (250 ft) telescope and the 256 channel autocorrelation spectrometer (Davies *et al.* 1969). No attempt was made to measure polarization; at 613 and 1425 MHz the feeds were linearly polarized while at 922 MHz the feed was circularly polarized. The beamwidths were $14' \times 19'$, $16' \times 22'$ and $31' \times 31'$ arc at 1425, 922 and 613 MHz respectively. At 1425 MHz the telescope was illuminated in such a way as to give maximum gain which resulted in a high sidelobe level ($\sim$ 10 dB down). At 613 and 922 MHz the sidelobes were more than 20 dB below the mainbeam response. The conversion

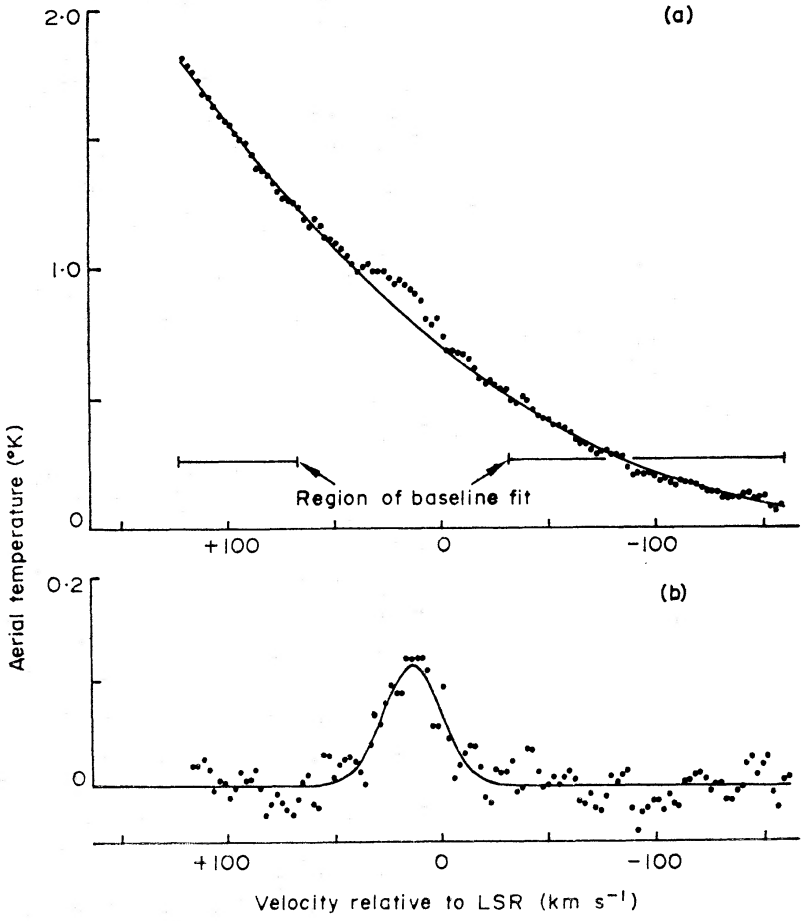

FIG. 1. *An illustration of the analytical technique of baseline removal by fitting a fourth-order polynomial to the observed spectrum outside the frequency range of the expected emission. (a) The spectrum after folding the original 256-point spectrum containing two profiles. The region of the spectrum to which the baseline was fitted is shown. (b) The final spectrum with the baseline removed.*

TABLE I

Westerhout number	H II region Optical object	Position l	b	RA (1950) h m s	Dec. (1950) ° ′	220α T_l (°K)	220α Δv (kHz)	220α v (km s^{-1} rel. to lsr)	192α T_l (°K)	192α Δv (kHz)	192α v (km s^{-1} rel. to lsr)	166α T_l (°K)	166α Δv (kHz)	166α v (km s^{-1} rel. to lsr)
W1	NGC 7822	118·2	+4·9	00 00 18	66 58	0·118±0·021	71±16	−10·8±3·9	—	—	—	—	—	—
W3	IC 1795	133·7	+1·2	02 21 45	61 53	0·159±0·023	55±8	−42·7±1·1	—	—	—	0·185±0·010	110·8	−40·7±0·8
W10	Orion Nebula	209·0	−19·4	05 32 49	−05 25	0·136±0·028	83±25	−7·2±4·4	0·168±0·019	113±15	−18·9±2·5	0·560±0·043	166±19	−4·2±1·3
W12	NGC 2024	206·5	−16·4	05 39 24	−01 52	<0·05	—	—	—	—	—	0·130±0·010	155±16	8·9±1·3
W16 (1)	Rosette	206·8	−1·8	06 30 30	04 38	0·114±0·018	63±14	13·3±2·4	—	—	—	—	—	—
W16 (2)	Nebula	206·1	−2·3	06 28 12	05 06	0·114±0·012	63±10	14·7±2·0	—	—	—	—	—	—
W29	M8, NGC 6523	6·0	−1·2	18 00 34	−24 22	0·307±0·019	70±6	2·8±1·5	—	—	—	0·247±0·021	152±19	8·5±1·4
W35	NGC 6604	18·5	+1·9	18 15 00	−11 52	0·344±0·022	70±6	28·1±1·1	—	—	—	0·157±0·011	189±30	34·0±2·1
W37	M16, NGC 6611	17·0	+0·8	18 15 55	−13 47	0·441±0·036	67±6	22·8±1·4	—	—	—	—	—	—
W37 (1)		16·9	+0·8	18 16 05	−13 52	—	—	—	—	—	—	0·175±0·016	193±26	28·2±1·6
W37 (2)		17·0	+0·9	18 15 40	−13 44	—	—	—	—	—	—	0·239±0·018	132±15	27·1±1·2
W38	M17, NGC 6618	15·1	−0·7	18 17 33	−16 12	0·344±0·039	96±19	15·2±3·6	0·290±0·020	125±10	10·3±1·5	0·892±0·031	223±10	20·9±0·7
W43		30·8	0·0	18 45 00	−01 59	0·538±0·060	80±12	95·0±1·5	0·243±0·027	113±8	92·4±1·3	0·323±0·017	174±11	99·0±2·1
W49		43·2	0·0	19 07 48	09 01	—	—	—	—	—	—	0·096±0·013	146±27	15·6±0·8
W51		49·0	−0·3	19 20 04	14 02	0·358±0·026	73±6	58·3±2·3	0·189±0·015	66±6	56·6±1·0	0·280±0·036	136±27	—
(DR23)		81·5	0·0	20 39 05	41 46	—	—	—	—	—	—	0·186±0·013	124±19	7·5±1·3
W80	NGC 7000	84·9	−0·8	20 53 24	43 52	0·160±0·021	53±10	1·8±2·3	—	—	—	0·074±0·007	181±42	4·2±2·4

(a) The values of T_l, Δv and v given for the 192α lines are effected by curved baselines; the errors given are 3SD and are determined from a gaussian fit only. The real errors may be several times those quoted. W10 has the most discordant velocity; it appears to be the result of baseline uncertainties.

(b) The velocities of all 166α lines appear to be approximately 4 km s^{-1} high when compared with other observations. The origin of this difference is unknown, but is believed to be the result of an offset of an LO which could not be traced after the observations. The W51 spectrum had an additional unexplained offset.

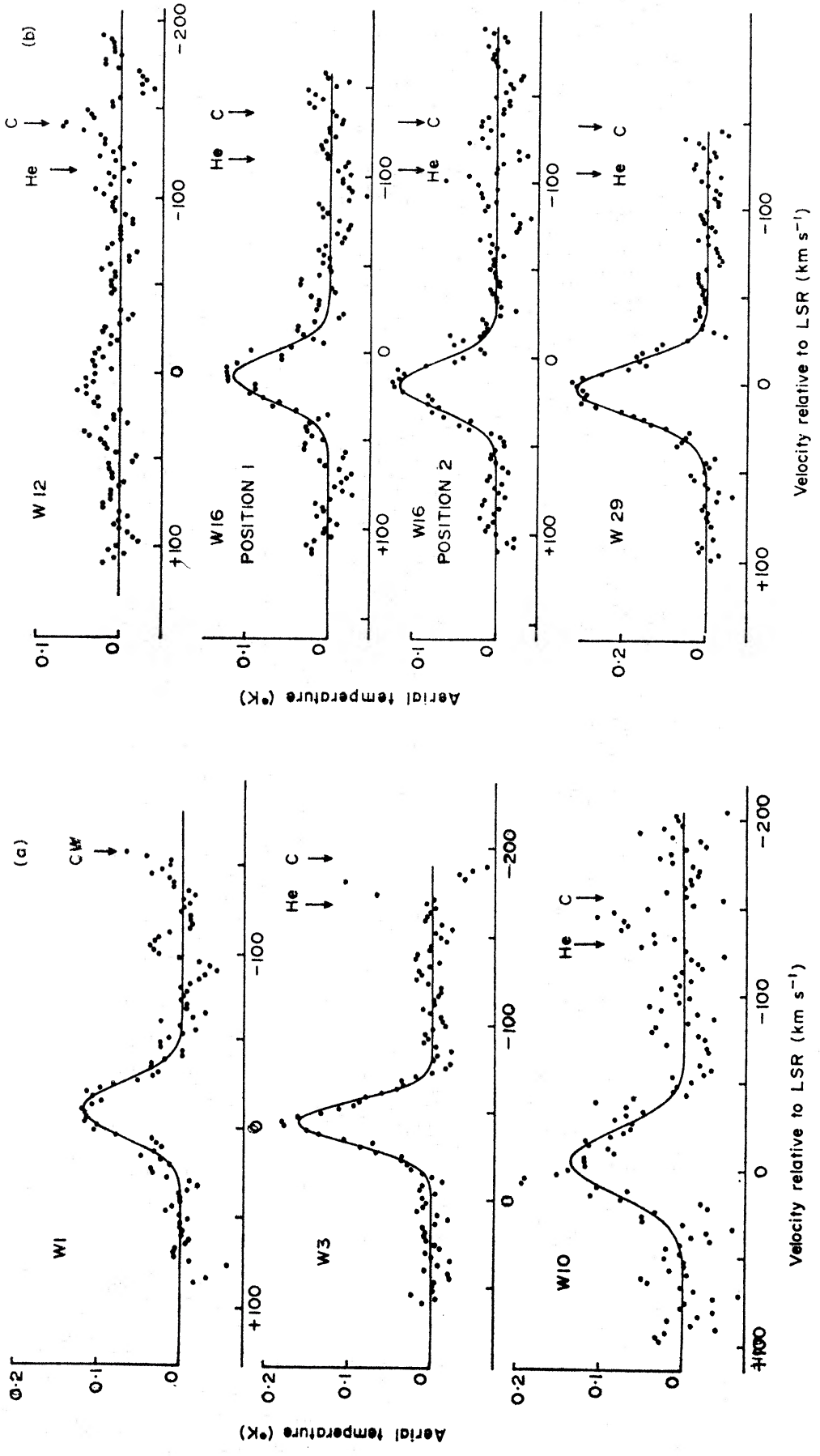

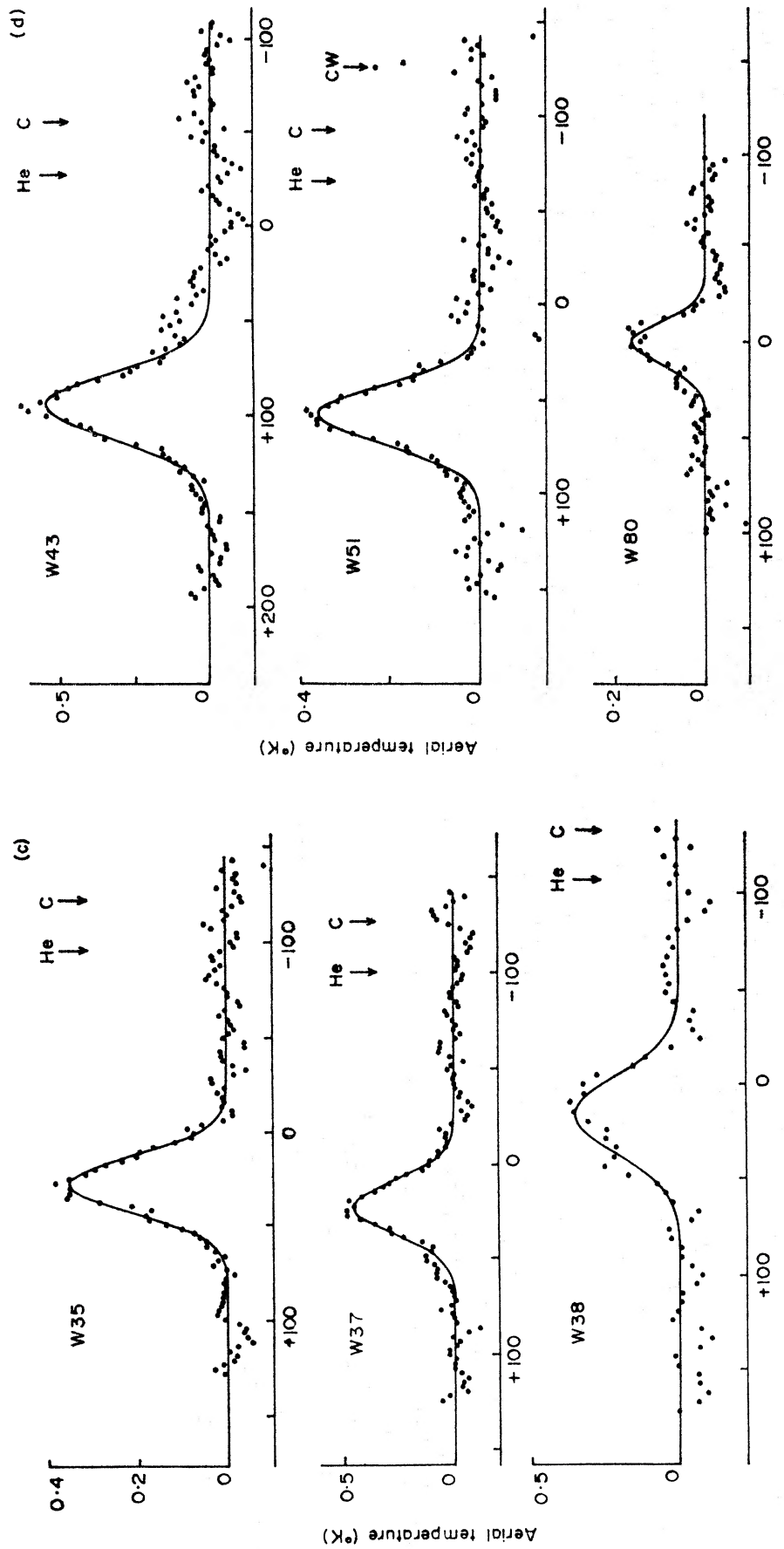

FIG. 2. *220α recombination line spectra of 13 H II regions. Zero velocity relative to the lsr is at 613·405 MHz; the beamwidth is 31′ × 31′ arc. The helium and carbon velocities of W12 are based on the hydrogen spectrum of Ball* et al. (1970). *The symbol CW on the W1 and W51 spectra denotes continuous wave interference.*

factor from flux density to aerial temperature was 2·15, 3·8 and 4·3 flux units per degree for 613, 922 and 1425 MHz. This calibration was based on a flux density of Cygnus A equal to 3550 f.u. at 613 MHz, 2300 f.u. at 922 MHz and 1460 f.u. at 1425 MHz (1 f.u. = 10^{-26} Wm^{-2} Hz^{-1}).

The receivers used parametric amplifiers as the first stages at all frequencies and in all cases the system noise was between 50 °K and 100 °K when the telescope was directed to cold sky. The receiving band containing the spectral line was converted to a video band between 0 and 5 MHz which was analysed by the autocorrelation spectrometer. During processing the autocorrelation function was multiplied by a triangular weighting function which gave a spectrometer frequency response of the form $(\sin x/x)^2$ with a half-power width of 1·8 channels and only 4 per cent sidelobes.

The power spectrum obtained in this manner consists of the recombination line superposed on the broadband continuum contribution from the H II region being observed as well as noise generated in the receiving system. The recombination lines measured at these wavelengths are considerably less than 1 per cent of these two contributions. Several methods of removing the broadband contributions were tried including taking reference spectra off the source and on a non-thermal source of similar intensity. The method which was found most satisfactory for this particular experiment was the frequency switching method in which the first local oscillator was switched over such a frequency range that the signal and reference spectra were in different halves of the video band. This method had the advantage of doubling the effective observing time compared with the other methods.

One is then left with the problem of removing the residual baseline after the 256-channel data for each source have been appropriately folded to produce a single spectrum which is the sum of the two spectra in the original. This was achieved by removing a fourth-order polynomial fitted to the data outside the frequency range of the expected line. An example of this procedure applied to the 220α line of W16 is shown in Fig. 1. The error introduced by this process was evaluated using the method described by Churchwell & Edrich (1970) and is included in the listing of the results in Table I. The approximate slope of the baselines removed were 1 °K in aerial temperature per MHz for the 166α and 220α lines and 10 °K per MHz for the 192α spectra. The greater slope in the latter spectra were the result of a much narrower parametric amplifier bandwidth which for various reasons could not be optimized at the time of these measurements. As a consequence there is a greater uncertainty in the baselines fitted to the 192α data.

After the baselines were removed from the observed spectra in the manner described above, gaussian profiles were fitted to the emission features. The amplitude of the line (T_l), its half-power width ($\Delta\nu$) and the velocity of the line centre were obtained for the best fitting gaussian in each case. These are given along with their errors in Table I. Positions and names of the various sources are included. The final spectra with their best fitting gaussians are shown in Figs 2, 3 and 4 for the 220α, 192α and 166α lines respectively.

3. THE SIZES OF THE H II REGIONS OBSERVED

The H II regions studied here were deliberately chosen to have a wide range of densities and as a consequence they have a wide range of angular sizes; the lowest

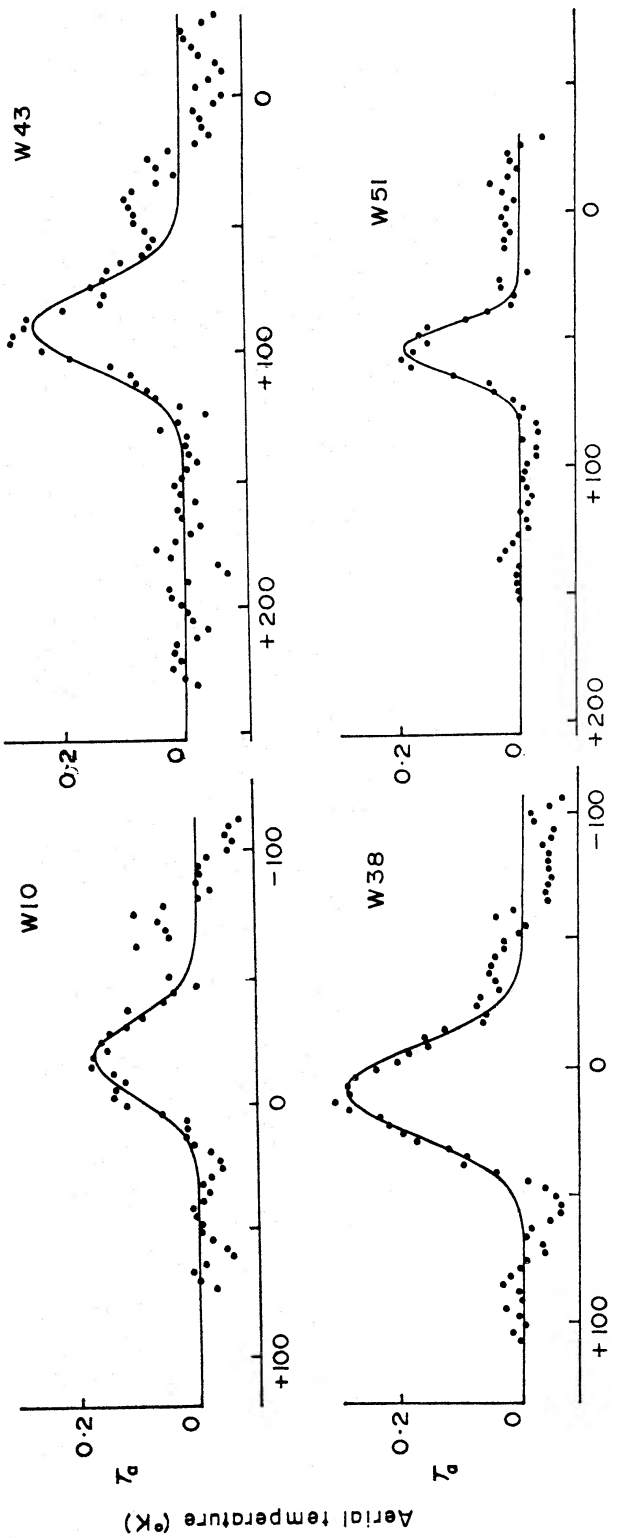

FIG. 3. 192α *recombination line spectra of* 4 *H* II *regions. Zero velocity relative to the lsr is at* 921·897 *MHz; the beam width is* 16′ × 22′ *arc.*

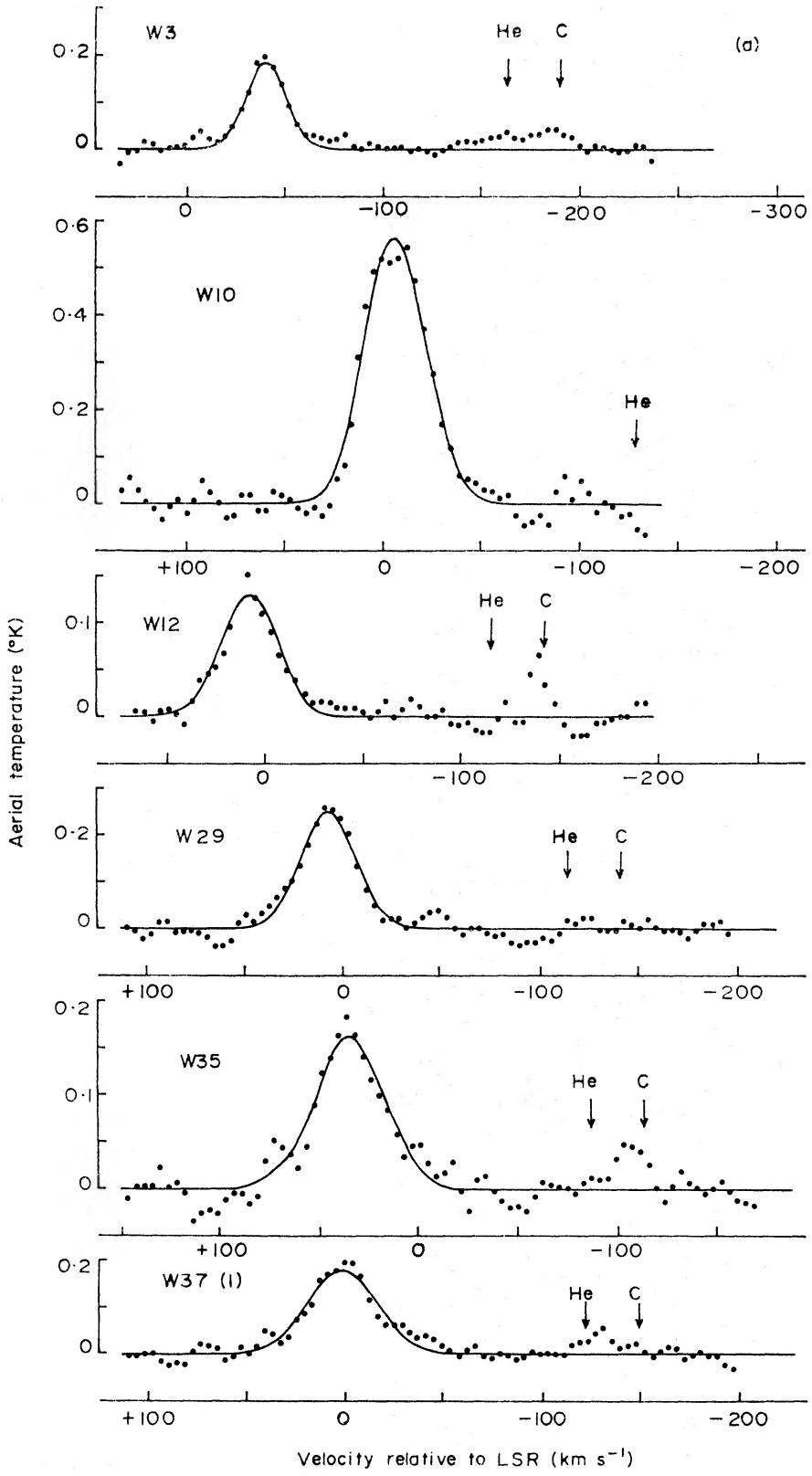

FIG. 4(*a*).

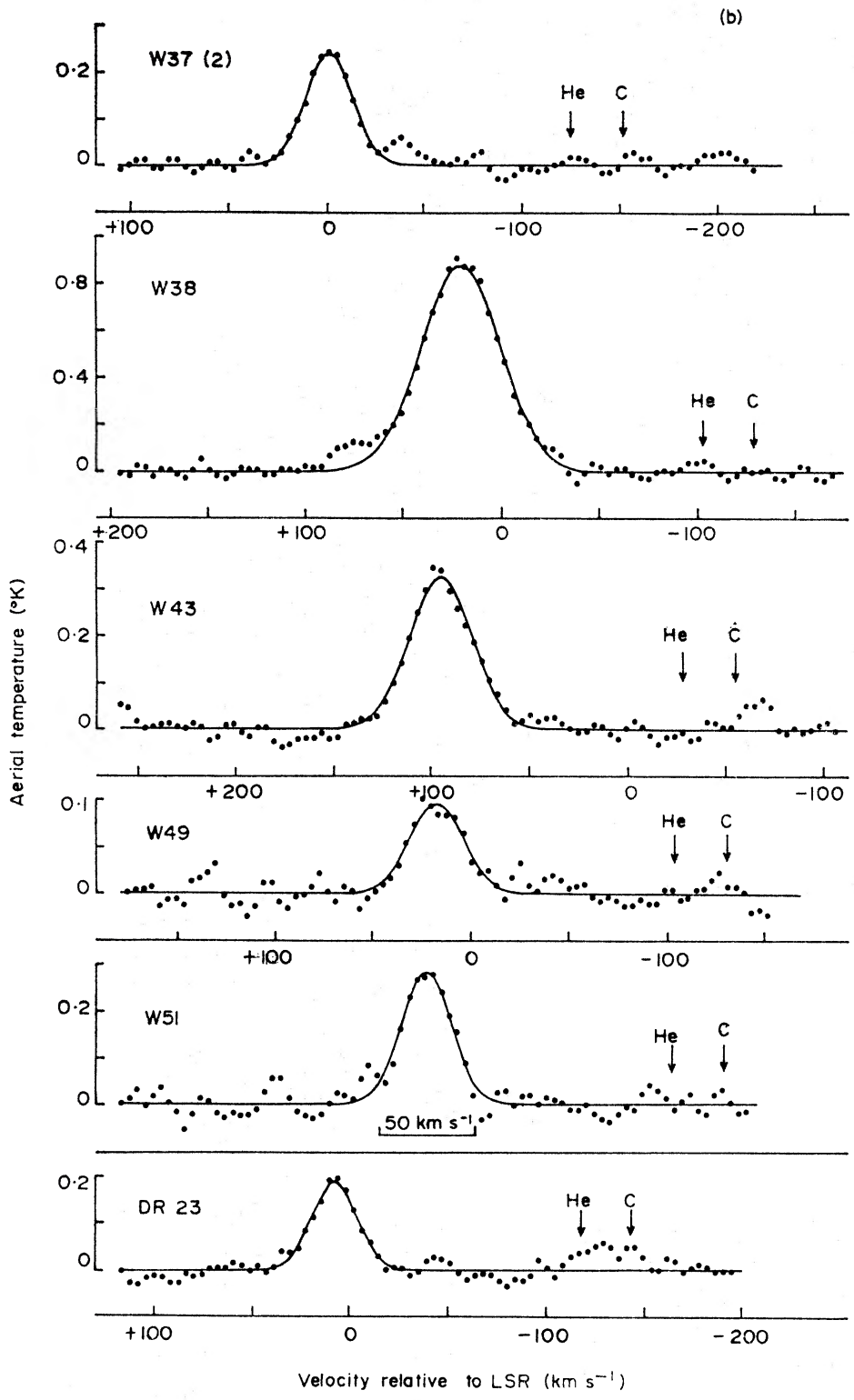

FIG. 4(*b*).

FIG. 4. 166α *recombination line spectra of* 12 *H* II *regions. Zero velocity relative to the lsr is at* 1424·734 *MHz; the beamwidth is* 14′ × 19′ *arc. No velocity scale is assigned to W*51 *because of an unrecorded LO setting.*

(a)

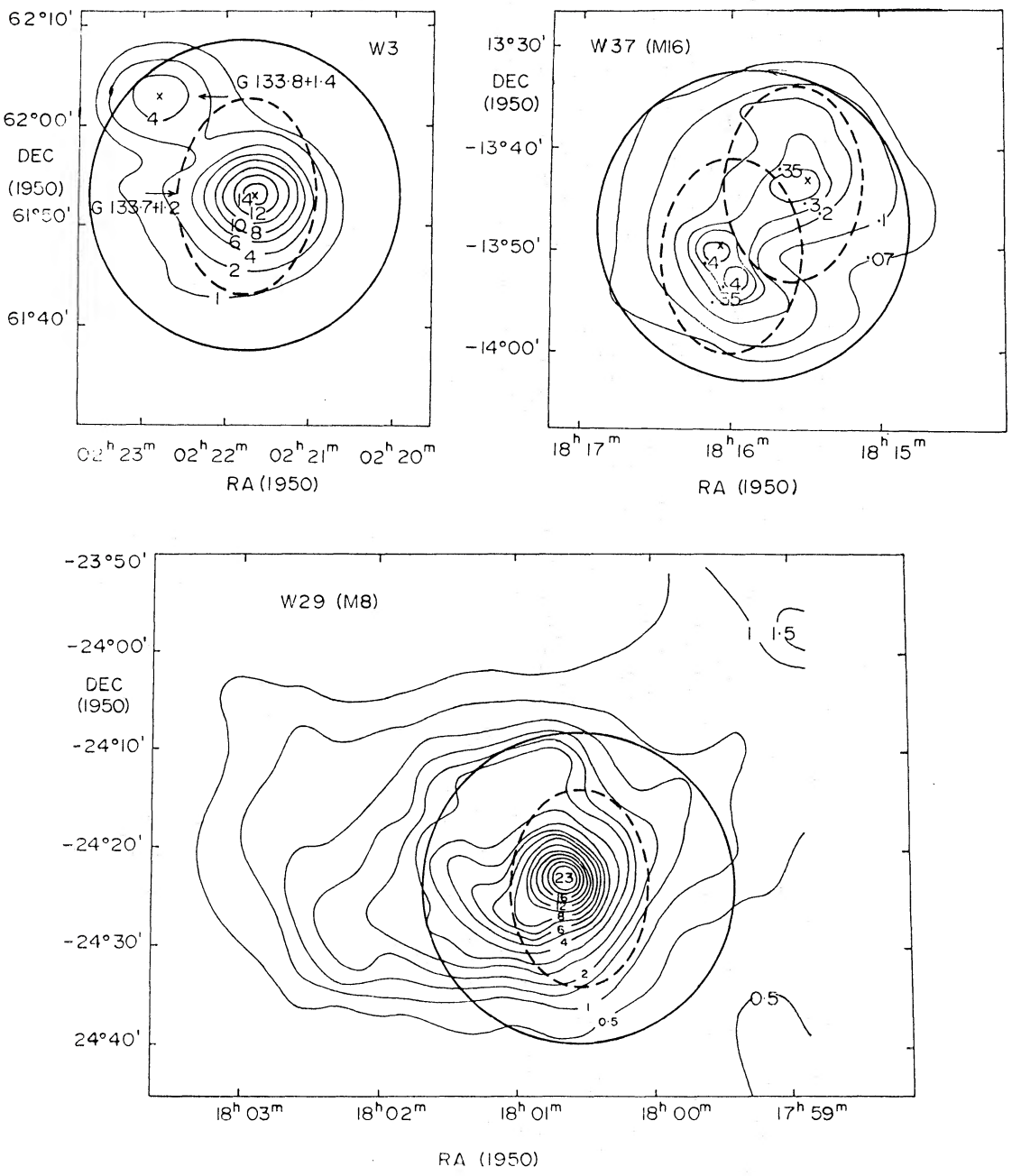

FIG. 5(*a*).

density objects have diameters of about 3° while the highest density objects are only a few minutes of arc in diameter. Since the beam area of the telescope at 613 MHz is approximately three times that at 1424 MHz the size of the source relative to the telescope beam is an important consideration in this experiment. In this connection the sources fall into three groups.

(*a*) *Sources smaller than the* 1424 *MHz* (166α) *beam*

This is the ideal situation for comparing the recombination line observations at different frequencies because the source is smaller than the beam in each case.

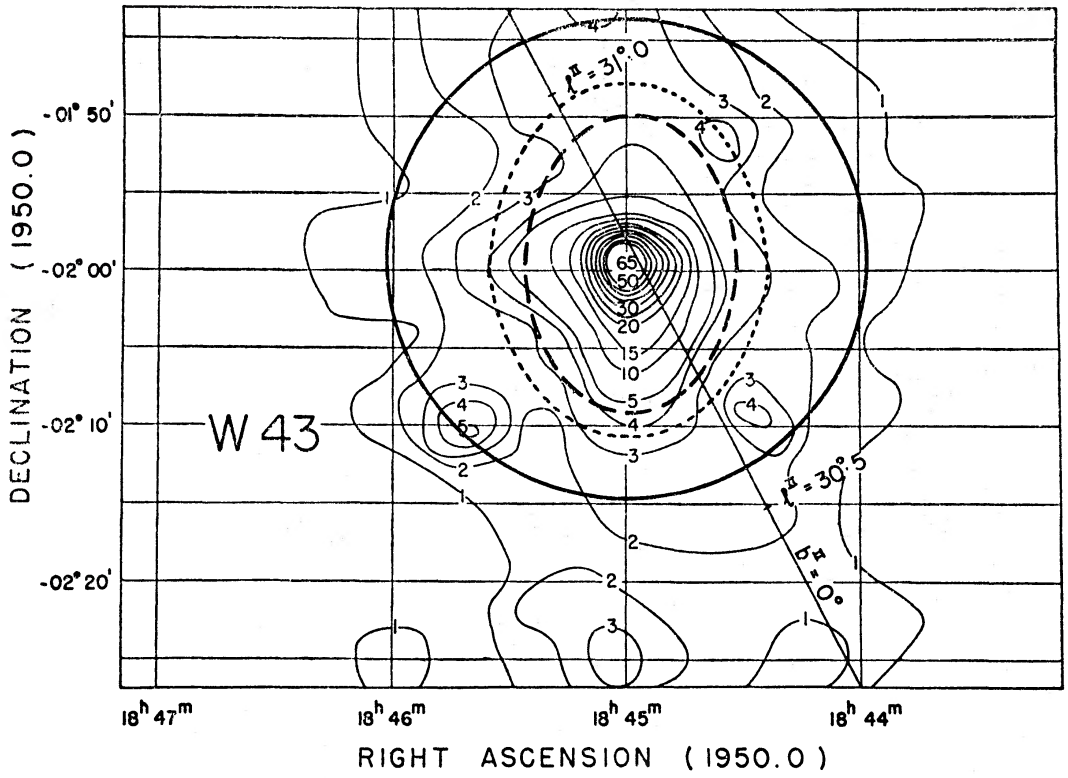

FIG. 5(*b*).

The sources in this category are W10 (Orion Nebula), W38 (M17) and W12 (NGC 2024). However all these sources are optically thick to varying degrees at decimetre wavelengths and hence comparisons between lines of different transitions must be made with caution as the lower frequency lines could be coming from the lower density parts of the source.

(*b*) *Sources larger than the 613 MHz beam*

This category includes W1 (NGC 7822), W16 (Rosette nebula), W35 and W80 (NGC 7000). The lines at different frequencies can be compared directly if the H II regions are homogeneous in electron density, emission measure and electron temperature over the area contained in the largest beam down to a scale size less than the smallest beam. In the case of W16 we have observed two regions in the 220α line separated by about 40′ arc and the two spectra were closely similar. However it is possible that all H II regions are not so homogeneous. For example Courtès, Louise & Monnet (1968) have shown that bright rims exist in W80 which have quite different electron temperatures and densities from the rest of the nebula.

(*c*) *Sources comparable in size with the telescope beams used*

The complex structure in the vicinity of many of the bright sources which can be isolated with the small beams used at high frequencies can complicate the observations at lower frequencies. Often a bright component is embedded in an extended low density region. W3 (IC 1795), W29 (M8), W37 (M16), W43 and W51 are of this type. Fig. 5 shows the beamwidths used in this investigation

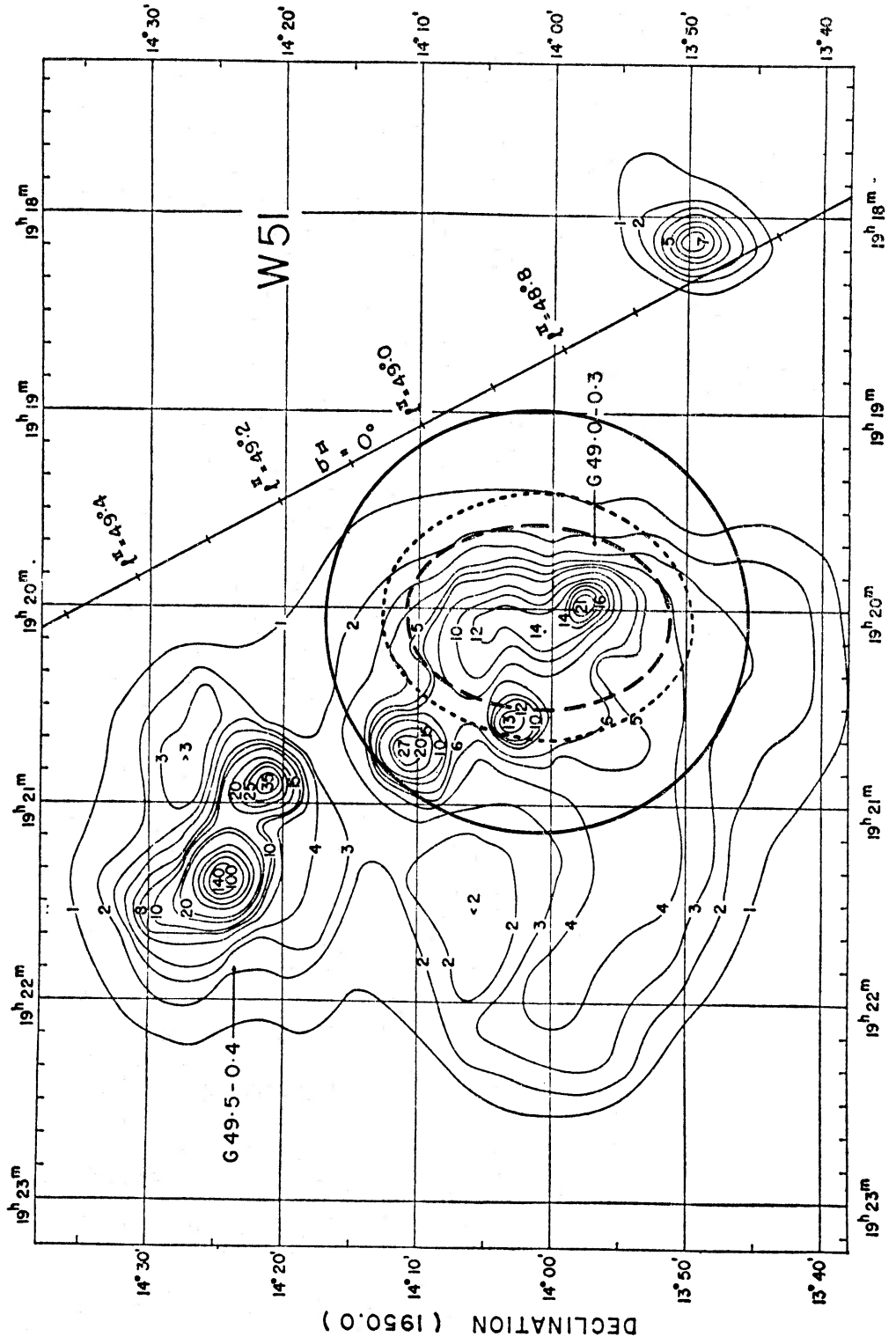

FIG. 5(c).

FIG. 5. Contour maps of W3, W29, W37, W43 and W51 with the beamwidths superposed. (W3 and W37 are from Mezger & Henderson 1967; W43 and W51 are from Macleod & Doherty 1968; W29 is from Goss & Shaver 1970). The 613 MHz beam is shown as a full line, the 922 MHz beam is dotted and the 1425 MHz beam is a broken line.

TABLE II

H II region	l	b	220α T_c (°K)	220α $\int T_l\,dv/T_c$ (kHz)	192α T_c (°K)	192α $\int T_l\,dv/T_c$ (kHz)	166α T_c (°K)	166α $\int T_l\,dv/T_c$ (kHz)	(a) N_e cm^{-3}	(a) Size
W1	118·2	+4·9	22·5	0·41 ± 0·08	—	—	2·5	—	~10	~2°
W3	133·7	+1·2	39·5	0·24 ± 0·04	—	—	14·7	1·79 ± 0·36	>2146	1·3′ × <0·7′
W10	209·0	−19·4	126·5	0·09 ± 0·03	84	0·24 ± 0·05	95	1·06★	2237	2·6′ × 3·5′
W12	206·5	−16·4	28·0	—	—	—	14·2	1·68 ± 0·35	1347	3·5′ × 1·9′
W16 (1)	206·8	−1·8	25·0	0·32 ± 0·08	—	—	—	—	13	1·3°
W16 (2)	206·1	−2·3	24·0	0·32 ± 0·06	—	—	—	—		
W29	6·0	−1·2	67·1	0·34 ± 0·06	—	—	20·1	2·14 ± 0·41	391	3·7′ × 3·0′
W35	18·5	+1·9	41·0	0·64 ± 0·10	—	—	8·5	3·90 ± 0·86	46	~0·6°
W37	17·0	+0·8	55·9	0·59 ± 0·09	—	—	—	—		
W37 (1)	16·9	+0·8	—	—	—	—	11·0	3·56 ± 0·50	87	4·9′ × 15·4′
W37 (2)	17·0	+0·9	—	—	—	—	11·0	3·62 ± 0·54		
W38	15·1	−0·7	166·8	0·20 ± 0·05	117	0·33 ± 0·07	10·2	2·21 ± 0·18	639	4·7′ × 2·4′
W43	30·8	−0·0	90·6	0·56 ± 0·07	38	0·75 ± 0·21	31·9	1·95 ± 0·23	301	1·7′ × 2·9′
W49	43·2	−0·0	—	—	—	—	12·1	1·30 ± 0·31	536	2·0′ × 1·0′
W51	49·0	−0·3	125·2	0·23 ± 0·04	41	0·32 ± 0·06	25·2	1·68 ± 0·29	238	1·8′ × 2·4′
DR23	81·5	+0·0	—	—	—	—	11	2·53 ± 0·41	~10^4	~0·5′
W80	84·9	−0·8	25·4	0·33 ± 0·10	—	—	4·6	3·40 ± 1·05	24	3·0° × 3·0

★ Inadequate frequency switch.

(a) Mainly taken from Schraml & Mezger 1969; these are merely indicative values of N_e and size.

superposed on contour maps of these five sources. In the case of W3 and W51 some emission sources are included in the 613 MHz beam which are not in the 1420 MHz beam, so comparisons between different frequencies for these H II regions must be made with caution.

The continuum aerial temperature, T_c, at the selected position in each H II region was measured from scans across the source in terms of a calibration signal and is listed in Table II. Since the recombination line temperature is measured in terms of the same calibration signal the ratio of the integral of the line profile to the continuum temperature, $\int T_l\, d\nu/T_c$, can be specified directly. This ratio for each line measured in the present observations is included in Table II.

It should be remarked that although we have expressed caution in comparing the recombination line spectra at different frequencies with different beam areas the information on line velocities given in Table I is encouraging. The velocities of the H II regions in Table I agree with the velocities given by Reifenstein *et al.* (1970) for the 109α line and by Dieter (1967) for the 158α line, confirming that we are observing at the various frequencies the same H II regions and not different regions in the same line of sight.

4. ELECTRON TEMPERATURES OF THE H II REGIONS

The calculation of an electron temperature from radio recombination line data was suggested by Kardashev (1960). It can be derived directly from the measured ratio of the integrated line profile to the continuum temperature using the following equation

$$\frac{\int T_l\, d\nu}{T_c} = \frac{3{\cdot}12 \times 10^{-12} \nu^{2{\cdot}1} T_e^{-1{\cdot}15}}{a(T_e, \nu)\left(1 + \dfrac{N(\text{He II})}{N(\text{H II})}\right)}$$

where $a(T_e, \nu)$ is a factor tabulated by Mezger & Henderson (1967), ν is the rest frequency of the line in Hz and $N(\text{He II})/N(\text{H II})$ is the ratio of the number of ionized helium to hydrogen atoms (which we shall assume to be 0·1). The use of this method of determining electron temperatures is based on the assumptions that (1) the levels are in local thermodynamic equilibrium (LTE), (2) the H II regions are optically thin and (3) the H II regions have a constant temperature throughout. The first assumption is not valid for most high density H II regions. However where the emission measure is less than 10^4 cm^{-6} pc and the electron density is greater than 10^2 cm^{-3} deviations from LTE will be small. Thus providing the densities in the regions of emission are greater than 10^2 cm^{-3} the recombination line data for the low brightness H II regions W1, W16, W35, W37 and W80 should give a good estimate of their electron temperatures. In cases where the continuum optical depth, τ_c, is appreciable (say $\geqslant 0{\cdot}1$) at 613 MHz the values of T_e derived from the observations should be corrected to T_e^1 by the relationship

$$T_e^1 = T_e \left(\frac{\exp(\tau_c) - 1}{\tau_c}\right)^{1/1{\cdot}15}.$$

In the low surface brightness H II regions discussed in this section the correction is small but it is important in all the other H II regions.

The values of T_e calculated from our data for these five H II regions are compared with other radio and optical estimates in Table III. Observations of the

radio continuum optical depth and brightness temperature also lead to a value of T_e (Shaver 1969, 1970). A direct optical method of determining T_e is to compare the Doppler widths of nitrogen and hydrogen lines (Dyson & Meaburn 1971). Another estimate of the temperature can be made from the ratio of intensities of the [N II] and H_β lines (Foukal 1969); these have been included in Table III for comparison.

The electron temperatures derived from the 220α observations of W1, W16

TABLE III

Electron temperatures in low brightness H II Regions

H II region	Recombination lines 220α (°K)	Recombination lines 166α (°K)	Radio continuum (Shaver 1969, 1970)	Optical line widths (Dyson & Meaburn)	Line intensity ratios (Foukal)
W1 (NGC 7822)	5400 ± 1000	—	—	—	—
W16 (Rosette)	6700 ± 1500	—	—	3610	—
W35	3700 ± 500	3600 ± 700	4000	—	—
W37 (M16)	3900 ± 500	3800 ± 500	5000	11850	10500
W80 (NGC 7000)	6600 ± 1700	—	—	4380* 5150	7800

* The values refer to two positions in the nebula, both of which are different from that used for the recombination line measurements.

and W80 fall between 5000 and 7000 °K whereas W35 and W37 have temperatures close to 4000 °K. The lower temperatures for these sources compare well with those obtained with the radio continuum method by Shaver (1970). It is possible that the low temperature obtained for W37 in the 220α and 166α transitions is a non-LTE effect since Reifenstein *et al.* obtained 6100 °K from 109α observations; W37 has the highest emission measure of the sources in Table III and may therefore be outside the range of emission measure compatible with LTE. The optical data do not show a very close agreement with the radio results. Apart from W37, they indicate temperatures lower than those generally found for higher density H II regions. It should be remembered that the optical measurements refer only to the brightest knots in the H II regions. Although there is a scatter in the values of T_e given in Table III we suggest that it does provide strong evidence from a number of approaches for electron temperatures in the range 4000 to 6000 °K in the low emission measure H II regions; these values are substantially lower than those found in higher density H II regions. This fall in electron temperature with decreasing density is in the sense expected for collisional deexcitation of the cooling ions.

5. NON-LTE EFFECTS

Apart from the H II regions discussed in the previous section, non-LTE effects are likely to be important and should be taken into account. The theoretical non-LTE analysis based on the calculation of b_n factors has been performed by several authors and their results are in essential agreement (e.g. Sejnowski & Hjellming 1969; Brocklehurst 1970). The application of these computations to recombination

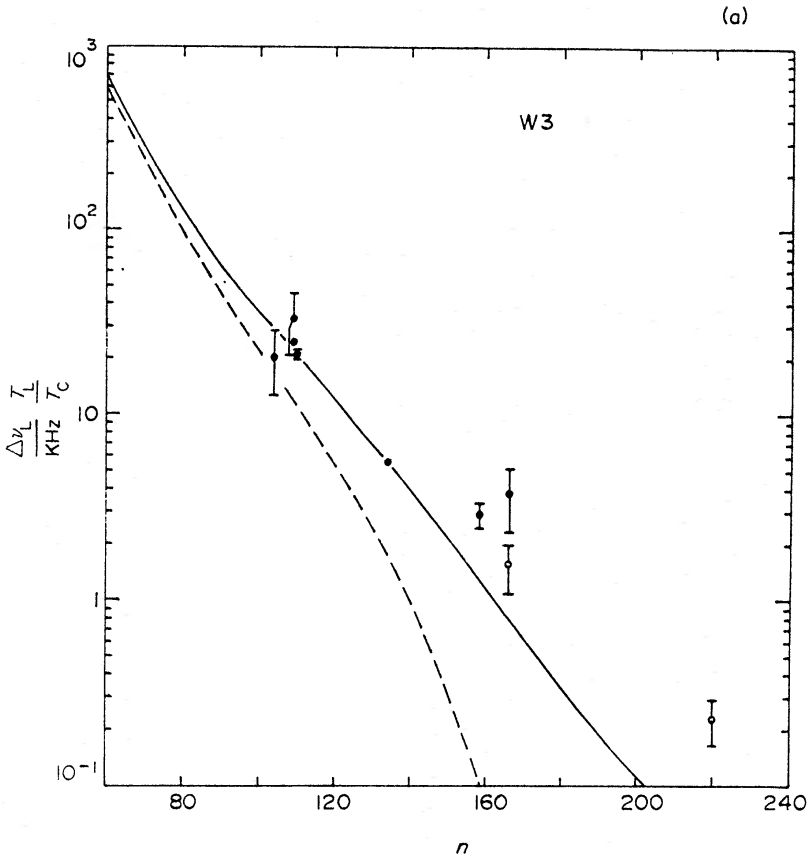

FIG. 6(*a*).

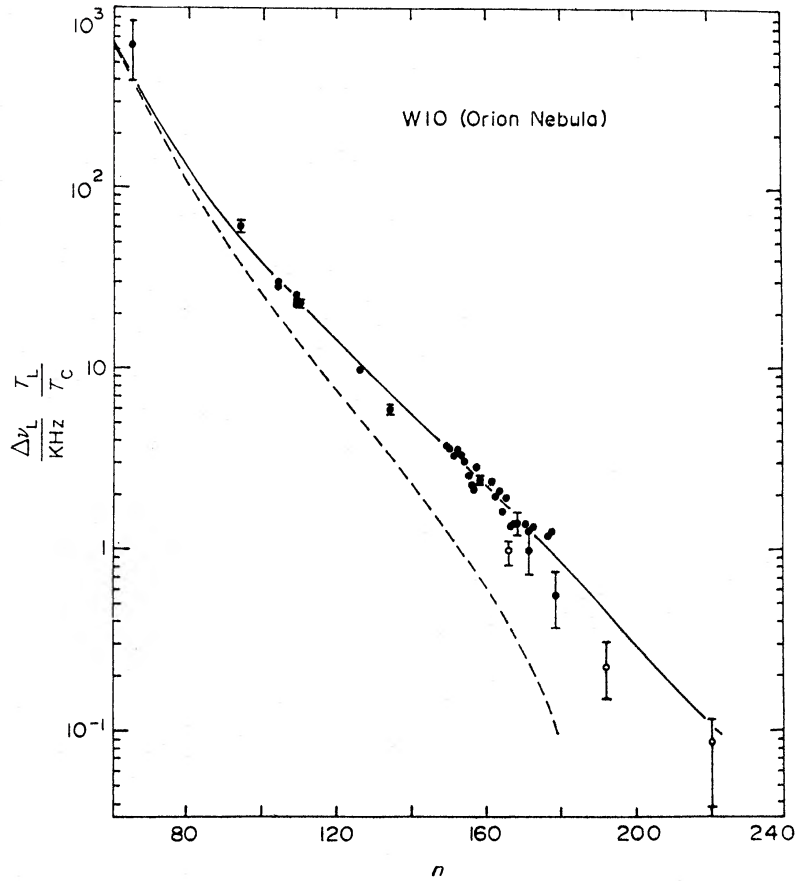

FIG. 6(*b*).

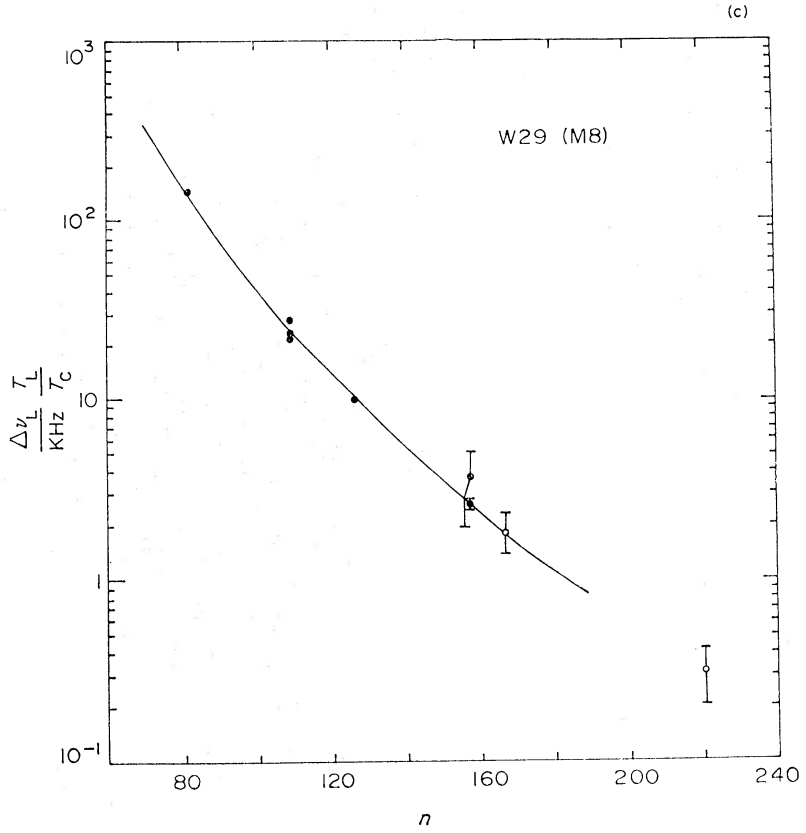

FIG. 6(*c*).

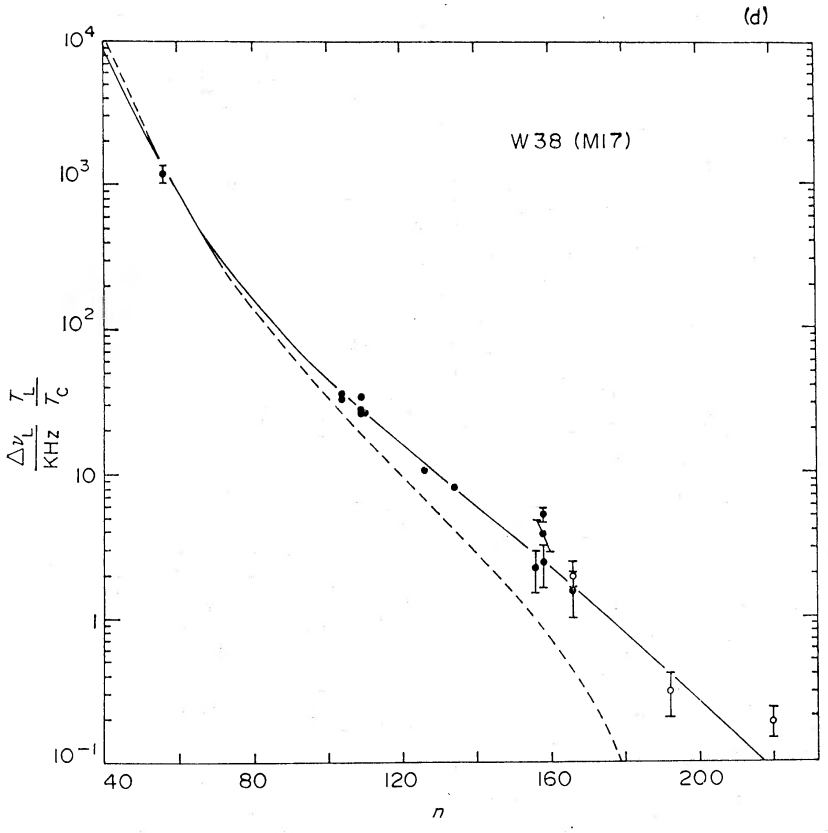

FIG. 6(*d*).

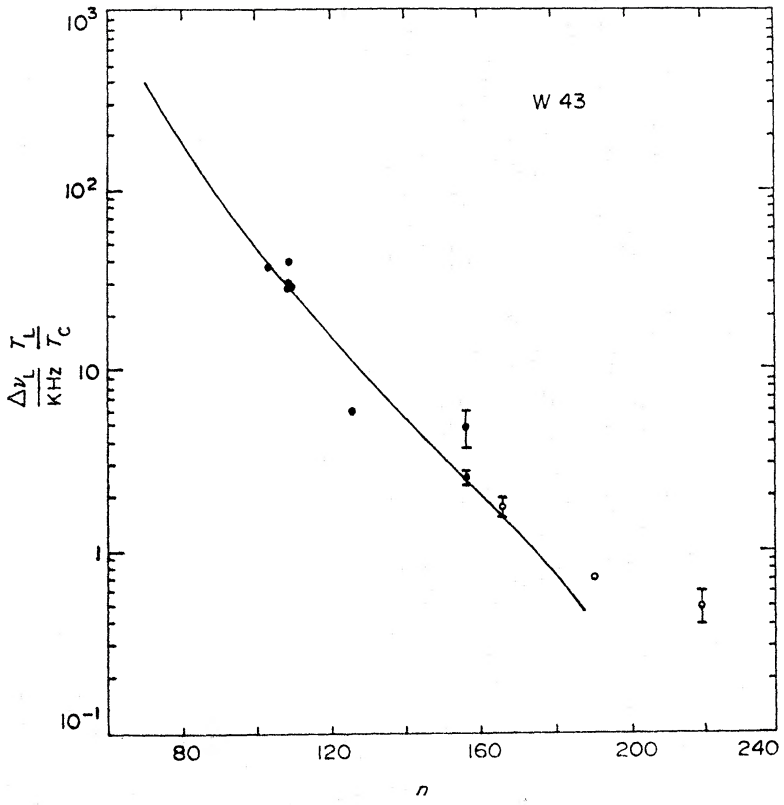

FIG. 6(*e*).

FIG. 6. 166α, 192α *and* 220α *observations of* $W3$, $W10$, $W29$, $W38$ *and* $W43$ *compared with* α*-transition observations at lower* n *values. In each case the observations are compared with a non-LTE solution (full line) and with an LTE solution (dotted) taken from Hjellming & Davies* (1970) *and from Andrews* et al. (1971). *The data obtained in the present investigation are shown as* ○.

line observations of a source over a range of n values and using α, β, γ, δ-transitions leads to an estimate of $\langle N_e \rangle$, $\langle T_e \rangle$ and $\langle E \rangle$ appropriately averaged over the source. The present observations provide a useful extension of the α-transition data to larger n values than have been used hitherto in non-LTE analyses.

Hjellming & Davies (1970) have found solutions to all the observations available to them for W3, W10, W38 and W51. Andrews, Hjellming & Churchwell (1971) have extended this analysis to W29, W43 and W49. The α-transition data are plotted for W3, W10, W29, W38 and W43 in Fig. 6 along with the best-fitting non-LTE solution for all the data (including β, γ, δ and ϵ transitions). The values of $\langle N_e \rangle$, $\langle T_e \rangle$ and $\langle E \rangle$ for the solutions are given in Table IV. Also plotted in Fig. 6 are the variations of $\int T_l \, d\nu / T_c$ against n which would have occurred under the assumption of LTE. The present observations have been included in the plots.

The 166α and 220α points fit the non-LTE predictions for W10 and W38 very well indicating that the data at these longer wavelengths are still consistent with the values of $\langle N_e \rangle$, $\langle T_e \rangle$ and $\langle E \rangle$ given in Table IV. For W3 the agreement is not so good; the observed value of $\Delta\nu T_l / T_e$ exceeds the predicted by ~ 5 times the error in the observation. This is not surprising as the area of W3 covered by the 613 MHz beam (see Fig. 5) includes regions of lower brightness (emission measure) and possibly lower electron temperature which have a higher value of

$\int T_l\, dv/T_c$. Also it can be seen that the present 166α point taken with a $14' \times 19'$ beam agrees better with the low n transitions than the 166α point of de Boer *et al.* which was observed with a 36′ arc beam and suffers in the same way as our 220α point. Unfortunately it is not possible to compare our 166α, and 220°α data for W51 with the non-LTE predictions of Hjellming and Davies as these refer to a different component of W51.

Brocklehurst & Seaton (1971) have made an independent examination of the recombination line data for Orion A and show that the present low frequency data are consistent with their analysis which includes the effects of non-LTE and Stark broadening.

TABLE IV

Non-LTE solutions of recombination line data (Hjellming & Davies 1970; Andrews et al. 1970) plotted in Fig. 6

H II region	$\langle N_e \rangle$ (cm^{-3})	$\langle T_e \rangle$ (°K)	$\langle E \rangle$ (cm^{-6} pc)
W3 (IC 1795)	$7{\cdot}7 \times 10^4$	11000	4×10^7
W10 (Orion Nebula)	$2{\cdot}5 \times 10^4$	10000	$1{\cdot}26 \times 10^7$
W29 (M8)	$4{\cdot}9 \times 10^3$	7700	$1{\cdot}0 \times 10^6$
W38 (M17)	$3{\cdot}8 \times 10^4$	8000	$1{\cdot}0 \times 10^7$
W43	$2{\cdot}1 \times 10^4$	7200	$9{\cdot}0 \times 10^6$

6. THE LINE PROFILE SHAPES

The broadening of recombination lines is caused principally by Doppler effects. For higher n values, however, pressure (Stark) broadening may be important. In an earlier paper (Pedlar & Davies 1971) we have shown that the effect is small for the 220α lines studied here and it should therefore be negligible for most of the 166α lines. Accordingly the 166α profiles should give a direct measure of the contributions to the Doppler broadening by thermal and turbulent (or larger scale) velocities. If a Maxwellian distribution of turbulent velocities, v_t, is assumed the half-power width, D, of a hydrogen recombination line is given by

$$D = \frac{2\nu}{c} \ln 2 \left[\left(\frac{2kT_e}{M_H} + \frac{2}{3}\langle v_t^2 \rangle\right)\right]^{1/2}$$

where ν is the line frequency, k is Boltzmann's constant, M_H is the mass of the hydrogen atom and $\langle v_t^2 \rangle$ is the mean square velocity. Values of the r.m.s. turbulent velocity $\langle v_t^2 \rangle^{1/2}$ calculated from this expression are given in Table V. Two estimates are given for each source; one is based on the electron temperature derived from the 166α data on the assumption of LTE and the other is based on an assumed value of 10^4°K. Since it is evident that the sources with higher emission measure are not in LTE an assumed temperature of 10^4°K leads to a reasonable estimate of the turbulent velocity. Further, since most H II regions have electron temperatures $< 10^4$°K the value of $\langle v_t^2 \rangle^{1/2}$ given in Table V will be, if anything, a lower estimate.

It can be seen that the majority of the H II regions have turbulent velocities averaged over the area of the beam greater than the speed of sound in the medium which ranges from 11·5 to 14·8 km s^{-1} for electron temperatures of 6000 to 10 000 °K This suggests the presence of shock fronts in the H II regions. It is quite possible that some of these values of turbulence include mass motions in the regions. W10 (the Orion nebula) has been shown to be rotating (Mezger & Ellis 1968; Gordon &

Meeks 1968) with velocities of a few km s^{-1}. Studies of W51 with a 4·0′ arc resolution show that the region at $l = 49{\cdot}0°$, $b = -0{\cdot}3°$ has several components whose velocities range over ± 3 km s^{-1} from the mean (Wilson *et al.* 1970). The rather larger values of $\langle v_t^2 \rangle^{1/2}$ obtained in the present survey compared with those obtained in higher angular resolution surveys at smaller n values (for example, Reifenstein *et al.* 1970; Davies 1971) suggest that ionized hydrogen adjacent to the

TABLE V

Turbulent widths of 166α lines

H II region	T_e (LTE assumed)	$\langle v_t^2 \rangle^{1/2}$ (km s^{-1})	T_e (assumed)	$\langle v_t^2 \rangle^{1/2}$ (km s^{-1})
W3 (IC 1795)	7000	11	10 000	1
W10 (Orion Nebula)	11000*	16*	10 000	20
W12 (NGC 2024)	8100	19	10 000	16
W29 (M8)	6000	20	10 000	17
W35	3600	27	10 000	25
W37 (1) } M16	3900	28	10 000	25
W37 (2) } M16	3800	18	10 000	13
W38 (M17)	5800	32	10 000	31
W43	6500	24	10 000	22
W49	(>9300)	—	10 000	16
W51	7400	16	10 000	14
DR 23	5200	16	10 000	11

* This measurement may be affected by the inadequate frequency separation of the reference frequency.

main emitting features may be contributing to the observed velocity spread. The 166α profile of W37 (1) shows significant deviation from a gaussian shape which agrees with that obtained in the 110α line observed by Davies. It should be emphasized that when all such departures from a gaussian distribution of turbulent velocities are taken into account, we are still left with a turbulent velocity component comparable with or greater than the speed of sound in most H II regions.

7. RECOMBINATION LINES FROM ELEMENTS OTHER THAN HELIUM

When an atom other than hydrogen emits a radio recombination line the transition occurs between outer orbitals from where the inner electron(s) can be assumed to shield the excess charge on the nucleus. The frequency of the recombination line between states n and n' of a species x is then given by the Rydberg relation with the Rydberg constant corrected for the different effective mass of the electron

$$\nu_x = \frac{R_\infty}{1 + \frac{M_e}{M_x}} \left(\frac{1}{n^2} - \frac{1}{(n')^2} \right)$$

where M_e and M_x are the masses of the electron and the element x. For carbon this results in a frequency shift relative to hydrogen of 150 km s^{-1}. For helium the shift is 122 km s^{-1}. The expected positions of the helium and carbon lines are marked on the spectra plotted in Figs 2, 3 and 4.

(*a*) *Helium recombination lines*

Several workers (Palmer *et al.* 1969; Churchwell & Mezger 1970; Davies 1971) have used the 109α and 110α transitions to obtain the relative abundance of helium to hydrogen in several H II regions. Most H II regions are found to emit helium recombination lines with an integrated intensity of ~10 per cent of the hydrogen 109α line. The present data allow us to see if this ratio changes for larger n-values.

The 166α spectra as a whole are consistent with a helium to hydrogen line ratio of 10 per cent. Values $\lesssim 5$ per cent are however found in W12 (NGC 2024) and W43 where similar low values have been observed previously in the 109α and 110α transitions. These low values have been interpreted as due to the possible smaller ionized helium zone around an ionizing star compared with the ionized hydrogen zone; this is a consequence of the higher ionization potential of helium. The central star of NGC 2024 is a B0·5 star (Garrison 1968) which is significantly less bright than an O7 star which Higgs & Ramana (1968) show is necessary to fully ionize both helium and hydrogen in an H II region.

Many of the 220α lines do not show significant helium lines although, because of the lower signal to noise ratios of these data and the baseline uncertainties, the limit cannot be set much below 10 per cent for many of the sources. Several sources (W3, W35, W37 and W51) seem to have helium lines less than this. It is possible that the apparent ratio of helium to hydrogen can fall at lower frequencies where the central regions of the H II regions become optically thick and as a result the helium emission from the central zone is attenuated; the hydrogen recombination line in such a situation would come mainly from the outer layers where helium is only partially ionized.

(*b*) *Recombination lines from heavier elements*

Recombination lines from elements heavier than helium would be expected, on the basis of their measured abundance in H II regions (e.g. Peimbert & Costero 1969), to be about 10^{-4} of the strength of the corresponding hydrogen recombination line. Palmer *et al.* (1967) discovered a feature on the 109α spectrum of NGC 2024 whose intensity was approximately 3 per cent of the hydrogen line and which corresponded to a mass $>9\,M_{\rm H}$. Similar features were later found in W3, W10, W51 (G49·5+0·4) and NGC 6367 which further confirmed that the line was from a heavy element. Goldberg & Dupree (1967) suggested that the element was carbon because of its relatively high abundance and proposed that the emission arose from an overpopulation of the upper levels resulting from dielectronic recombination.

Our longer wavelength observations (Pedlar 1970) of NGC 2024 in the 166α line showed that the carbon line was of comparable intensity to the hydrogen line. Our 220α line spectra of the Orion nebula and NGC 2024 indicate the presence of a carbon line signal. Although some interference was present in the 220α observations it appeared not to affect the spectra of these two sources in the vicinity of the carbon line. Our values of the line temperature in the carbon line are compared with other observations (Palmer *et al.* 1969; Zuckerman & Palmer 1970; Churchwell & Edrich 1970; Ball *et al.* 1970; Davies 1971), for W3, W10 W12 and W43 in Table VI. The variation of the line to continuum ratio with n for carbon is compared with the ratio for hydrogen in W12 (NGC 2024) in Fig. 7. It can be seen that the carbon line peak temperature is only a few per cent of the hydrogen line

TABLE VI

Peak values of the aerial temperature for carbon lines expressed as a fraction of the continuum temperature for $W3$, $W10$, $W12$ and $W43$

Source	94α[1]	109α[2]	110α[3]	134α[4]	157α[5, 6]	166α[7]	168α[8]	192α[7]	220α[7]
W3	—	0·0035	—	0·0050	0·0052	<0·0040	0·0035	—	—
W10	—	0·0014	—	0·0014	0·0024	—	0·0010	—	0·0008
W12	0·0078	0·0093	—	0·010	0·010	0·0056	—	0·0034	0·0021
W43	—	—	0·0024	—	<0·0007	<0·0030	—	—	—

1. Chaisson 1971.
2. Palmer *et al.* 1969.
3. Davies 1971.
4. Zuckerman & Palmer 1970.
5. Churchwell & Edrich 1970.
6. Ball *et al.* 1970.
7. Present observations.
8. Simpson 1970.

at $n \simeq 100$ and becomes comparable to, and possibly exceeds, the hydrogen line at $n \simeq 200$.

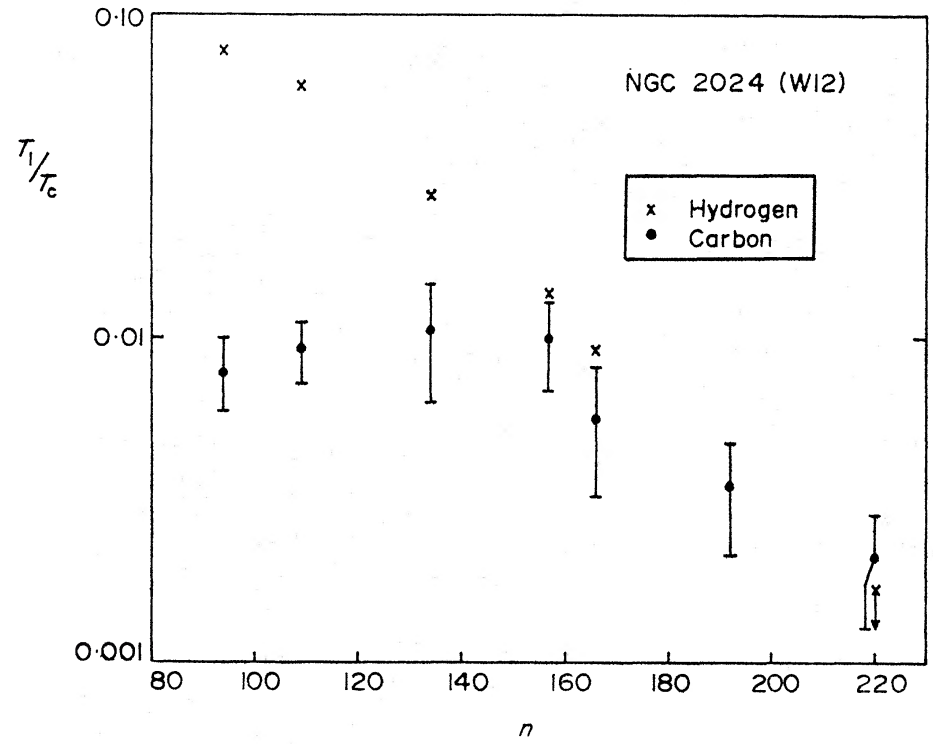

FIG. 7. *The ratio of the peak line temperature to the continuum temperature for W12 (NGC 2024) in the carbon and hydrogen lines. The 166α, 192α and 220α data are from the present observations.*

This variation of carbon line intensity with n is incompatible with the dielectronic recombination explanation of Goldberg and Dupree. Alternative models have been proposed which envisage that the carbon line originates in an H I region. Zuckerman & Palmer (1968) postulated that the H I region lies within the H II region. This explanation meets difficulty in the case of W10 (Orion Nebula) where at 613 MHz the centre is optically thick and the 220α carbon line emission would be expected to be heavily attenuated. However uncertainties in b_n factors at low temperatures make assertions regarding the intensity of the expected carbon lines somewhat uncertain (Dupree 1971; Percival & Seaton 1972). Dupree & Goldberg (1968) suggested that these carbon line H I regions of low density lie in front of the H II regions emitting the hydrogen recombination line. Evidence for this model has been advanced by Ball *et al.* (1970) who claim to have observed, superposed on the hydrogen recombination line, the H I emission corresponding to the carbon line in the 157α profile of W12. The present 166α data for W12, although taken with inadequate frequency resolution to fully resolve the emission from the H I region, show some asymmetry which is consistent with the interpretation of Dupree & Goldberg (1968).

CONCLUSIONS

The present observations have illustrated the range of problems which can be investigated by using observations of high quantum number (low frequency)

recombination lines. Although the lines are weak and are difficult to detect, they are particularly useful in providing answers to the following problems.

(*a*) *The search for Stark broadening*

Since the broadening is proportional to n^7, observations at the lowest feasible frequencies give the best chance of detecting the effect and thereby giving a direct estimate of the electron density N_e. Since the effect has already been shown to be small in the α lines, observations at similar frequencies in the β, lines are now required.

(*b*) *The investigation of non-LTE effects in radio recombination lines*

Observations over a wide range of n give the best opportunity to solve for $\langle N_e \rangle$, $\langle T_e \rangle$ and $\langle E \rangle$ in any H II region, following the approach of Hjellming & Davies (1970).

(*c*) *The understanding of the anomalous recombination lines*

Our observations show that these lines dominate the recombination line spectrum in some H II regions at large n values. Observations of the ratio of β to α lines will provide a critical test of the models proposed to explain these lines (Dupree 1971).

(*d*) *The zoning of ionized helium and hydrogen in H II regions*

The present observations indicate that at low frequencies, where the central regions of some dense H II regions are optically thick, the emission from the outer regions shows a deficiency of ionized helium. This result should be pursued further observationally.

(*e*) *The investigation of low surface brightness (emission measure) H II regions*

Since the ratio of the recombination line to the continuum temperature $T_l/T_c \propto \lambda^{-1}$ and $T_c \propto \lambda^{-2.1}$ then the recombination line strength $T_l \propto \lambda^{1.1}$. Low brightness H II regions are therefore best investigated at low frequencies. Furthermore, as shown in a previous section, such regions are likely to be in LTE. As a consequence T_e and E can be derived directly from the observations.

ACKNOWLEDGMENTS

We wish to thank Drs G. de Jager, R. S. Booth, A. J. Wilson and Mr M. R. W. Masheder for assistance with the observing and Dr C. J. Salter for help with the analysis. We are grateful to Drs M. Brocklehurst, J. E. Dyson, J. Meaburn and Professor M. J. Seaton for helpful discussions. A.P. acknowledges financial support from the Science Research Council during the tenure of a Studentship and a Research Fellowship.

University of Manchester, Nuffield Radio Astronomy Laboratories, Jodrell Bank

REFERENCES

Andrews, M. H., Hjellming, R. M. & Churchwell, E., 1971. *Astrophys. J.*, **167,** 245.
Ball, J. A., Cesarsky, D., Dupree, A. K., Goldberg, L. & Lilley, A. E., 1970. *Astrophys. J.*, **162,** L25.
Boer, J. A. de, Hin, A. C., Schwartz, U. J. & Woerden, H. van, 1968. *Bull. astr. Inst. Nethl.*, **19,** 460.
Brocklehurst, M., 1970. *Mon. Not. R. astr. Soc.*, **148,** 417.
Brocklehurst, M. & Seaton, M. J., 1971. *Astrophys. Lett.*, **9,** 139.
Chaisson, E. J., 1971. *Astrophys. J.*, **170,** 81.
Churchwell, E. & Edrich, J., 1970. *Astr. Astrophys.*, **6,** 261.
Churchwell, E. & Mezger, P. G., 1970. *Astrophys. Lett.*, **5,** 189.
Courtès, G., Louise, R. & Monnet, G., 1968. *Ann. Astrophys.*, **31,** 493.
Davies, R. D., 1971. *Astrophys. J.*, **163,** 479.
Davies, R. D., Ponsonby, J. E. B., Pointon, L. & Jager, G. de, 1969. *Nature*, **222,** 933.
Dieter, N. H., 1967. *Astrophys. J.*, **150,** 435.
Dupree, A. K., 1971. *Astrophys. J.*, **170,** L119.
Dupree, A. K. & Goldberg, L., 1968. *Astrophys. J.*, **158,** L49.
Dyson, J. E. & Meaburn, J., 1971. *Astr. Astrophys.*, **12,** 219.
Foukal, P., 1969. *Astrophys. Space Sci.*, **5,** 469.
Garrison, R. F., 1968. *Publ. astr. Soc. Pacific*, **80,** 20.
Goldberg, L. & Dupree, A. K., 1967. *Nature*, **215,** 41.
Gordon, M. A. & Meeks, M. L., 1968. *Astrophys. J.*, **152,** 417.
Goss, W. M. & Shaver, P. A., 1970. *Aust. J. Phys., Astrophys. Suppl. No.* **14.**
Higgs, L. A. & Ramana, K. V. V., 1968. *J. R. astr. Soc. Canada*, **62,** 5.
Hjellming, R. M. & Davies, R. D., 1970. *Astr. Astrophys.*, **5,** 53.
Kardashev, N. S., 1960. *Sov. Astr. — Astr. J.*, **3,** 813.
Macleod, J. M. & Doherty, L. H., 1968. *Astrophys. J.*, **154,** 833.
McGee, R. X., Batchelor, R. A., Brooks, J. W. & Sinclair, M. W., 1969. *Aust. J. Phys.*, **22,** 631.
Mezger, P. G. & Ellis, S. A., 1968. *Astrophys. Lett.*, **1,** 159.
Mezger, P. G. & Henderson, A. P., 1967. *Astrophys. J.*, **147,** 471.
Palmer, P., Zuckerman, B., Penfield, H., Lilley, A. E. & Mezger, P. G., 1967. *Nature*, **215,** 40.
Palmer, P., Zuckerman, B., Penfield, H., Lilley, A. E. & Mezger, P. G., 1969. *Astrophys. J.*, **156,** 887.
Pedlar, A., 1970. *Nature*, **226,** 830.
Pedlar, A. & Davies, R. D., 1971. *Nature*, **231,** 49.
Peimbert, M. & Costero, R., 1969. *Bol. Obs. Tonantzintla Tacbaya*, **31,** 3.
Penfield, H., Palmer, P. & Zuckerman, B., 1967. *Astrophys. J.*, **148,** L25.
Percival, I. C. & Seaton, M. J., 1972. *Astrophys. Lett.*, **11,** 31.
Reifenstein, E. C., Wilson, T. L., Burke, B. F., Mezger, P. G. & Altenhoff, W. J., 1970. *Astr. Astrophys.*, **4,** 357.
Schraml, J. & Mezger, P. G., 1969. *Astrophys. J.*, **156,** 269.
Sejnowski, T. J. & Hjellming, R. M., 1969. *Astrophys. J.*, **156,** 915.
Shaver, P. A., 1969. *Mon. Not. R. astr. Soc.*, **142,** 273.
Shaver, P. A., 1970. *Astrophys. Lett.*, **5,** 167.
Simpson, J. P., 1970. *Astrophys. Lett.*, **7,** 43.
Wilson, T. L., Mezger, P. G., Gardner, F. F. & Milne, D. K., 1970. *Astrophys. Lett.*, **5,** 99.
Zuckerman, B. & Palmer, P., 1968. *Astrophys. J.*, **153,** L145.
Zuckerman, B. & Palmer, P., 1970. *Astr. Astrophys.*, **4,** 244.